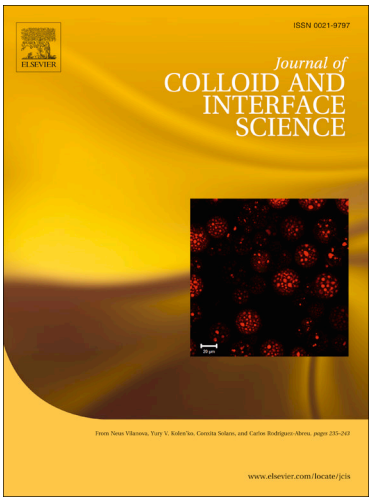

Long-Term Creep Deformations in Colloidal Calcium–Silicate–Hydrate Gels by Accelerated Aging Simulations

Han Liu, Shiqi Dong, Longwen Tang, N.M. Anoop Krishnan, Enrico Masoero, Gaurav Sant, Mathieu Bauchy

PII: S0021-9797(19)30187-0
DOI: https://doi.org/10.1016/j.jcis.2019.02.022
Reference: YJCIS 24646

To appear in: *Journal of Colloid and Interface Science*

Received Date: 16 October 2018
Revised Date: 24 December 2018
Accepted Date: 6 February 2019

Please cite this article as: H. Liu, S. Dong, L. Tang, N.M. Anoop Krishnan, E. Masoero, G. Sant, M. Bauchy, Long-Term Creep Deformations in Colloidal Calcium–Silicate–Hydrate Gels by Accelerated Aging Simulations, *Journal of Colloid and Interface Science* (2019), doi: https://doi.org/10.1016/j.jcis.2019.02.022

Graphical abstract

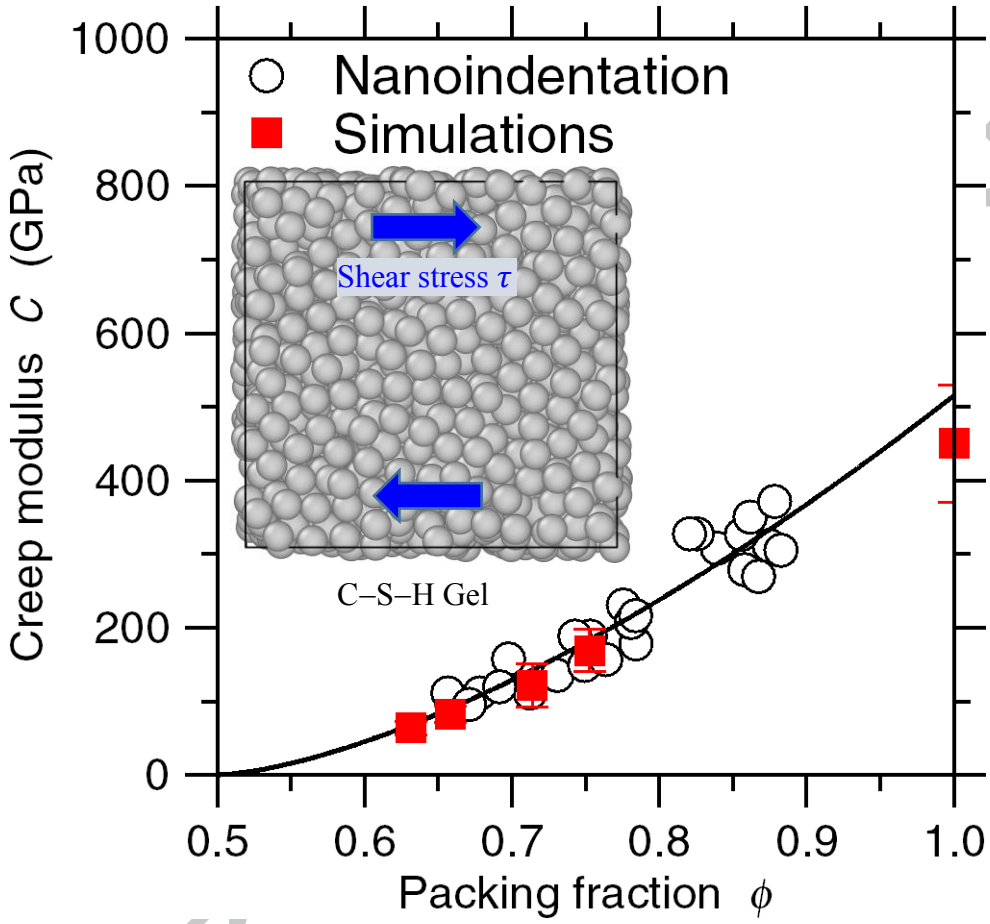

Long-Term Creep Deformations in Colloidal Calcium–Silicate–Hydrate Gels by Accelerated Aging Simulations

Han Liu [a], Shiqi Dong [a,b], Longwen Tang [a,c], N M Anoop Krishnan [a,d], Enrico Masoero [e], Gaurav Sant [b,f], Mathieu Bauchy [a,]*

[a] Physics of AmoRphous and Inorganic Solids Laboratory (PARISlab), Department of Civil and Environmental Engineering, University of California, Los Angeles, California, 90095, USA

[b] Laboratory for the Chemistry of Construction Materials (LC^2), Department of Civil and Environmental Engineering, University of California, Los Angeles, California, 90095, USA

[c] State Key Laboratory of Water Resources and Hydropower Engineering Science, Wuhan University, Wuhan 430072, China

[d] Department of Civil Engineering, Indian Institute of Technology Delhi, Hauz Khas, New Delhi 110016, India

[e] School of Engineering, Newcastle University, Newcastle Upon Tyne NE1 7RU, U.K.

[f] California Nanosystems Institute (CNSI), University of California, Los Angeles, California, 90095, USA

* Corresponding author: bauchy@ucla.edu

Keywords: Creep, Colloidal Gel, Accelerated Dynamics, Calcium–Silicate–Hydrate

Abstract

When subjected to a sustained load, jammed colloidal gels can feature some delayed viscoplastic creep deformations. However, due to the long timescale of creep (up to several years), its modeling and, thereby, prediction has remained challenging. Here, based on mesoscale simulations of calcium–silicate–hydrate gels (C–S–H, the binding phase of concrete), we present an accelerated simulation method—based on stress perturbations and overaging—to model creep deformations in C–S–H. Our simulations yield a very good agreement with nanoindentation creep tests, which suggests that concrete creep occurs through the reorganization of C–S–H grains at the mesoscale. We show that the creep of C–S–H exhibits a logarithmic dependence on time—in agreement with the free-volume theory of granular physics. Further, we demonstrate the existence of a linear regime, i.e., wherein creep linearly depends on the applied load—which establishes the creep modulus as a material constant. These results could offer a new physics-based basis for nanoengineering colloidal gels featuring minimal creep.

Introduction

Jammed colloidal gels—i.e., aggregated systems made of interacting nanograins [1,2]—are widely used in many industrial fields [3–5]. When subjected to a sustained load, jammed colloidal gels can feature some delayed viscoplastic creep deformations that can ultimately result in macroscopic failure [6–8]. Specifically, creep deformations in calcium–silicate–hydrate (C–S–

H) gels—the glue of concrete that forms upon the hydration of cement [5,9,10]—can decrease the lifespan of concrete structures [11–15]. This is significant as the maintenance or replacement of structures impacted by creep involves the use of large quantities of cement and concrete, which come with a significant environmental burden [6,16–18]. As such, the prediction of long-term creep deformations in C–S–H (and colloidal gels in general) could facilitate the design of new binders featuring minimal creep.

However, although various models have been proposed to explain the origin of concrete creep [11,15,19–22], the prediction of long-term creep deformations remains challenging. This arises from the facts that (i) cement binders are complex, multi-scale materials [5,9,23], (ii) various scales (atomic, mesoscale, etc.) may contribute to controlling creep [12], and (iii) creep deformations are associated with extended timescales, which far exceed the timescale accessible to conventional computional simulation methods (e.g., molecular dynamics or coarse-grained mesoscale simulations) [6,24,25].

To overcome the timescale limitation of conventional physics-based simulations techniques, we recently showed that stress perturbations cycles can be efficiently used to accelerate the aging of disordered, out-of-equilibrium materials [6,24,26]. Here, building on these ideas, we report some accelerated simulations of creep deformations in C–S–H based on the mesoscale model introduced by Masoero *et al.* [5]. We obtain a very good agreement with nanoindentation creep tests, which suggests that the reorganization of C–S–H grains at the mesoscale controls the creep of concrete. Based on these results, we show that the creep of C–S–H increases logarithmically with time, which is in line with experimental results from nanoindentation and with the predictions from the free-volume dynamics theory of granular physics [11,27]. Further, we establish the existence of a linear regime wherein creep deformations linearly depend on the

applied load, which allows us to define a "creep modulus" material constant. These findings could offer a new physics-based basis for nanoengineering colloidal gels featuring minimal creep.

This paper is organized as follows. In Sec. 2, we describe the methodology used herein to generate the C–S–H mesoscale configurations and model their creep deformations. In Sec. 3, we validate out simulations based on nanoindentation data and investigate the nature of creep deformations in C–S–H. Some consequences in the mechanism of creep in C–S–H are discussed in Sec. 4. Finally, some conclusions are presented in Sec. 5.

Methods

Preparation of the C–S–H configurations. We adopt here the colloidal model of C–S–H introduced by Masoero *et al.* [5,28], as it has been found to offer a realistic description of the mesoscale structure and nanomechanics of C–S–H [5,28,29]. In this model, the C–S–H gel is described as an ensemble of polydisperse spherical grains that interact with each other via a generalized Lennard-Jones interaction energy potential:

$$U_{ij}(r_{ij}) = 4\varepsilon(\sigma_i, \sigma_j)\left[\left(\frac{\bar{\sigma}_{ij}}{r_{ij}}\right)^{2\alpha} - \left(\frac{\bar{\sigma}_{ij}}{r_{ij}}\right)^{\alpha}\right] \quad \textbf{(Eq. 1)}$$

where σ_i and σ_j are the diameters of grains i and j, $\bar{\sigma}_{ij} = (\sigma_i + \sigma_j)/2$ is the average diameter for a given pair of atom, α is a parameter that controls the narrowness of the potential well, r_{ij} is distance between the centers of the grains i and j, and $\varepsilon(\sigma_i, \sigma_j)$ is the depth of the potential energy well. By considering each pair of grains in contact as two springs in series, the depth is given by $\varepsilon(\sigma_i, \sigma_j) = A_0\beta_{ij}{\bar{\sigma}_{ij}}^3$, where $A_0 = kE$ is a prefactor that is proportional to the bulk Young's modulus E of a grain, wherein $k = 0.002324$ (computed by the serial spring model) and $E = 63.6$ GPa (based on previous atomistic simulations of bulk C–S–H) [28,30]. $\beta_{ij} =$

$\sigma_i\sigma_j/\bar{\sigma}_{ij}{}^2$ is a correction term arising from the serial arrangement. The potential defined in Eq. 1 shows a minimum at $r_m = \sqrt[\alpha]{2}\bar{\sigma}_{ij}$ so that the effective diameter of a grain i is defined as $\sigma_{0,i} = \sqrt[\alpha]{2}\sigma_i$. The attractive force is maximum at a distance $r_u = \sqrt[\alpha]{\frac{4\alpha+2}{\alpha+1}}\bar{\sigma}_{ij}$ so that, by choosing $\alpha = 14$, the tensile strain at failure $\varepsilon_u = (r_u - r_m)/r_m$ is close to the value of 5% obtained in previous atomistic simulation of bulk C–S–H [28,30,31].

The C–S–H configurations are generated by grand canonical Monte Carlo (GCMC) simulations, as described in the following [5,29,32]. Starting from an initially empty cubic box with a size ranging from 600 to 920 Å, some C–S–H grains are iteratively inserted, wherein the size of each grain is randomly selected from a uniform distribution between a minimum σ_m and a maximum σ_M value. Experimentally, the polydispersity of the C–S–H grains is strongly supported by the absence of a clear characteristic size in SANS neutron scattering [9]. The standard deviation θ of the distribution is then used to define the polydispersity index of the configuration as: [5,28]

$$\delta = \theta/[(\sigma_m + \sigma_M)/2] \qquad \textbf{(Eq. 2)}$$

Here, various polydispersity values are considered, with σ ranging from 3.0 to 35 nm, and the number of grains at saturation ranging from 1700 to 7000. In detail, each GCMC step comprises 5 attempts of grain insertions or deletions followed by 500 attempts to randomly displace an existing grain. At each step, the probability of acceptance of the attempt is given by $\min\{1, \exp[-(\Delta U - \mu\Delta N)/k_B T]\}$ [33–35], where k_B is the Boltzmann constant, T the temperature, ΔU the variation in potential energy caused by the trial move, ΔN the variation in the number of C–S–H grains, and μ the chemical potential, which is taken here as $-2k_B T$ based on previous studies [34]. This value ensures the formation of a realistic final structure within a reasonable

simulation time. Note that, here, the chemical potential does not bear a quantitative meaning and that small variation in the chemical potential do not significantly alter the structure and properties of the simulated C–S–H samples [33,34]. This process is iteratively repeated until the number of inserted grains reaches a plateau. Note that the GCMC process is performed at constant volume—so that some tensile pressure builds up in the system upon precipitation. At the end of the GCMC simulation, such pressure is released by subjecting the system to a molecular dynamics relaxation in the *NPT* ensemble at zero stress, eventually followed by a final energy minimization. The packing fraction ϕ of each configuration is then computed as $\phi = [\sum_i((\pi/6)\sigma_{0,i}{}^3)]/V$, where V is the volume of the simulation box. Note that five independent simulations of C–S–H precipitation are performed for each degree of polydispersity to calculate the mean value and standard deviation of all the properties presented in the following.

In agreement with previous simulations [5,36], we observe that the C–S–H models that exhibit higher degrees of polydispersity eventually reach higher final packing fraction values—as small grains are able to fill the space left in between larger grains (see Fig. 1). For monodisperse configurations, the packing fraction at saturation is found to be around 0.63, that is, close to the theoretical packing limit of random monodisperse spheres [37,38]. Further, we note that the evolution of the packing fraction at saturation with polydispersity is in good agreement with the range of data observed in previous simulations [5,36].

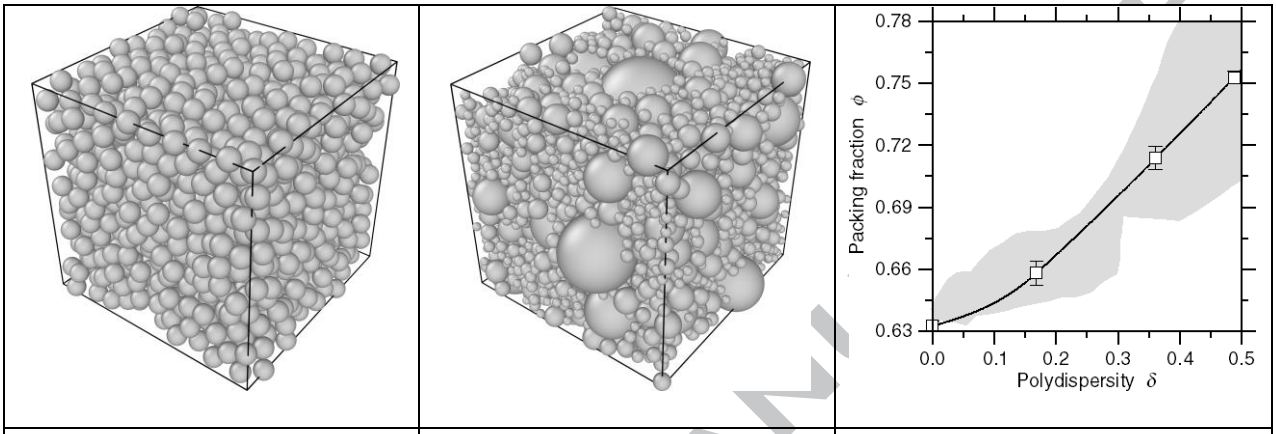

(a) **(b)** **(c)**

Fig. 1: Snapshots of select (a) monodisperse (polydispersity index $\delta = 0$, see Eq. 2) and (b) polydisperse C–S–H gel configurations ($\delta = 0.49$). (c) Computed packing fraction (at saturation) of the C–S–H gel configurations as a function of the polydispersity index. The grey area indicates the range of data observed in previous simulations [5,36].

Accelerated aging simulation methodology. We now focus on the methodology introduced herein to simulate creep. As mentioned above, the long-term nature of creep deformations far exceeds the typical timescale accessible to (coarse-grained) molecular dynamics simulations (i.e., from nano- to microseconds at most). Although kinetic Monte Carlo simulations could, in theory, describe the dynamics of the system over up to a few seconds, the application of this technique to polydisperse colloidal gels is challenging due to the high mobility of the small grains—which results in the existence of a large number of small energy barriers [25]. As such, the direct

simulation of the stress-induced creep deformation dynamics of C–S–H is, at this point, unachievable.

To overcome this limitation, we present here an accelerated simulation technique that is inspired by previous studies focusing on the relaxation of disordered atomic networks [6,24,26]. Refs. [24,26] provide some technical details on our accelerated method and offer an enthalpy landscape interpretation to the acceleration in the system dynamics that our technique yields. This technique relies on the application of small stress perturbations, which can accelerate the relaxation of out-of-equilibrium materials. Here, to simulate creep under sustained deviatoric load, the mesoscale C–S–H configurations are subjected an average shear stress τ_0 combined with small, cyclic perturbations of shear stress $\pm\Delta\tau$ (see Fig. 2). At each stress cycle, a minimization of the energy is performed, with the system having the ability to deform (shape and volume) in order to reach the target stress.

This method is inspired by the artificial aging and rejuvenation experienced by granular materials subjected to vibrations [39]. Namely, small vibrations can induce a compaction of granular materials, making the system *overage*. In contrast, large vibrations tend to randomize the grain configuration, which decreases the overall compactness and, therefore, makes the system *rejuvenate*. Similar ideas, relying on the energy landscape framework [7,8], have been applied to amorphous solids—based on the idea that an external stress tends to deform the energy landscape locally explored by the atoms. The application of a small external stress can result in the removal of some energy barriers existing at zero stress, thereby allowing some atoms to jump toward a new energy basin and relax to lower energy states. This transformation is irreversible as, once the stress is removed, the system remains in its aged state. In contrast, the application of a large stress can make the system move far from its initial state, which eventually

leads to rejuvenation—i.e., similar to thermal annealing [40]. As such, a succession of many of such small stress perturbations can be used to simulate the delayed relaxation of a disordered configuration subjected to a sustained load, i.e., creep.

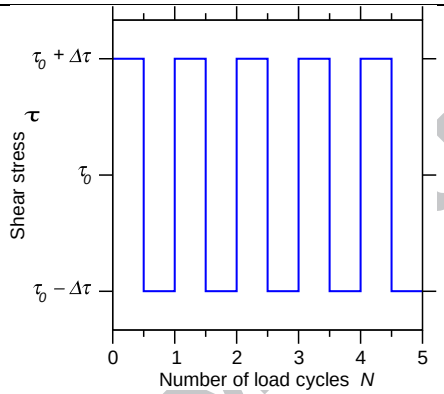

Fig. 2: Schematic presenting the stress perturbation cycles applied during our accelerated aging simulation method, where τ_0 is the average shear stress (i.e., causing the creep deformation of the colloidal C–S–H gel) and $\Delta\tau$ is the amplitude of the stress perturbations.

Results

Logarithmic nature of creep in C–S–H. Figure 3 shows the evolution of the shear strain γ of select C–S–H systems—under a sustained shear stress τ_0—obtained using our accelerated simulation method. Overall, we observe that the application of the stress cycles results in a gradual increase in shear strain. Note that, at zero average shear stress (i.e. $\tau_0 = 0$ MPa) no noticeable shear strain occurs (see Supplemental Material). Further, we note that γ increases

logarithmically with the number of applied stress cycles N and linearly with the applied stress τ_0. This suggests that the shear strain induced by creep can be expressed as:

$$\gamma(N) = (\tau_0/C)\log(1 + N/N_0) \quad \textbf{(Eq. 3)}$$

where C is the creep modulus and N_0 a fitting parameter that is analogous to a relaxation time [6,11]. Note that the number of load cycles N has been demonstrated to be equivalent to a fictitious time t, that is, $t = N\Delta t$, wherein Δt is a constant duration corresponding to each stress cycle [6,24,26]. This arises from the fact that the height of the energy barriers through which the system transits across each cycle, remains roughly constant over successive cycles [6] (see Supplemental Material). As such, on the basis of transition state theory, the time needed for a system to jump over an energy barrier E_A is constant and proportional to $\exp(-E_A/kT)$, where k is the Boltzmann constant and T the temperature [41]. However, the fictitious time associated with each stress cycle cannot be directly mapped into real time. In other words, we cannot ensure the trajectory of the C–S–H grains predicted by our accelerated simulation method is fully equivalent to the one that would be observed upon spontaneous creep. However, we previously demonstrated that macroscopic properties (e.g., strain), which are not very sensitive to the microscopic details of the system, exhibit a realistic evolution with the fictitious time [6]. The logarithmic nature of C–S–H creep observed herein is in good agreement with nanoindentation data [11,42] and such a logarithmic evolution has also been observed in the creep of various materials [43,44]. Similarly, a logarithmic compaction is also found in granular materials that are subjected to vibrations [39].

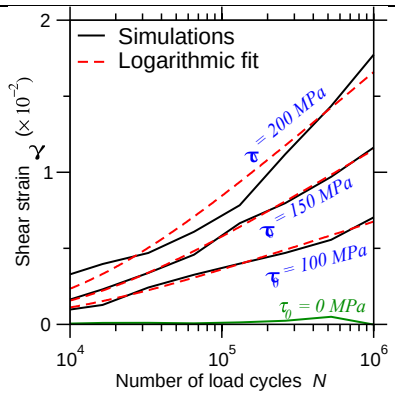

Fig. 3: Computed shear strain in monodisperse colloidal C–S–H gels with respect to the number of stress perturbation cycles N and for select average shear stress τ_0 values. The amplitude of the stress perturbations $\Delta\tau$ is here set as 30 MPa. The dashed lines are some logarithmic fits following Eq. 3.

Linear regime and creep modulus as a material constant. We now focus on the dependence of the shear strain γ on the applied shear stress τ_0. As expected, we observe that the magnitude of the creep-induced deformation increases with increasing values of applied load (see Fig. 3). The relationship between γ and τ_0 is effectively captured by the value of the creep modulus C—which should be constant if γ increases linearly with τ_0. Note that monodisperse C–S–H configurations and small stress perturbation values (here taken as 30 MPa) are first considered in this section.

Figure 4a presents the evolution of the creep modulus, which is obtained by fitting the strain curves such as those presented in Fig. 3 by the logarithmic law given in Eq. 3. Interestingly, we observe that, at low τ_0 values, the value of the creep modulus is constant and does not depend on τ_0. However, we note that the value of the creep modulus drastically decreases once the applied shear stress τ_0 exceeds a critical value (which is here found to be around 320 MPa). Note that, in

the low-stress regime, the N_0 constant is also found to be constant, which indicates that the mapping between number of stress cycles and corresponding creep time does not depend on the applied load.

Importantly, the fact that the creep modulus exhibits a constant value upon the application of low loads suggests that, under this regime, creep deformations feature a linear dependence on the applied load (see Eq. 3), in agreement with nanoindentation data [11,42]. This observation also establishes the creep modulus as an intrinsic material constant, that is, that only depends on the material composition and structure [6]. In addition, the linear nature of creep observed herein strongly supports the fact that, despite the large difference in length and time scales, small-scale creep deformations obtained by nanoindentation (obtained over a few seconds) should yield similar values of creep modulus than macroscopic creep tests (obtained over much longer periods of time).

Limits of the linear regime. We now investigate the origin of the departure from the linear regime at large stress (see Fig. 4a). To this end, Fig. 4b shows stress–strain behavior of monodisperse C–S–H under shear—wherein the C–S–H configuration is subjected to a pure shear deformation by gradually increasing the shear stress and performing an energy minimization after each increment of stress. As expected, we observe that, at low stress, shear stress increases linearly with shear strain, which characterizes a linear elastic deformation. We note that the system starts to exhibit some yielding around 600 MPa, which manifests itself by a deviation from linearity in the stress–strain curve and the existence of a residual permanent strain upon unloading. Based on this result, we conclude that creep remains linear as long as the applied load remains low as compared to the yield point of the material. These results echo the

conclusions of a previous study, wherein it was found that a mathematical condition to have a constant creep modulus C is that the activation energy for the irreversible rearrangements increases as the logarithm of the shear strain—a condition that was found to be valid only when the applied stress is lower than the yield stress [45]. Here, the present results suggest that the linear regime of creep extends up to stress values that are about 60% of the yield stress threshold. This can be understood from the fact that, when the load approaches the yield point, the material starts to experience local yielding, which results in a drop in creep modulus—i.e., a drastic increase in creep compliance (see Fig. 4a).

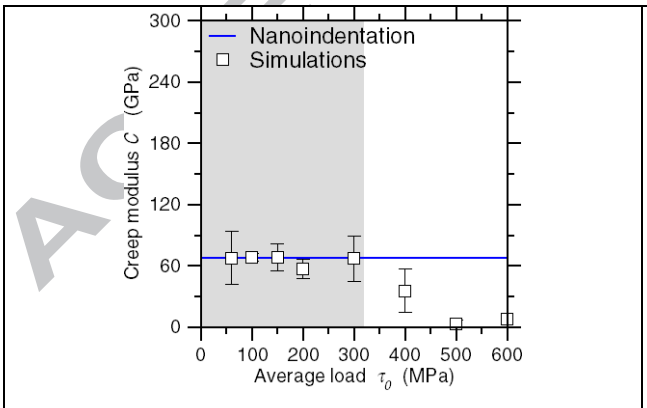

(a)

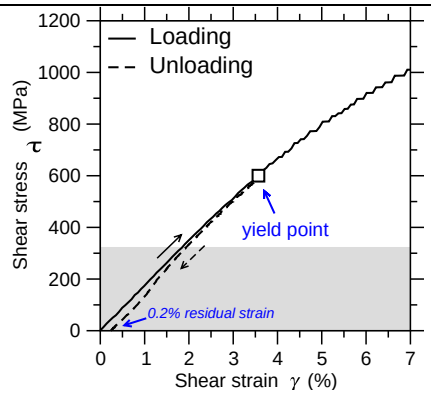

(b)

Fig. 4: (a) Computed creep modulus *C* (see Eq. 3) in monodisperse colloidal C–S–H gels under varying average shear stress values τ_0 (for $\Delta\tau$ = 30 MPa). The results are compared with experimental nanoindentation data (blue line) [11,42]. (b) Computed stress–strain curve in a monodisperse colloidal C–S–H gel upon shearing. The dash line is an unloading curve from the yield point (square point), where the residual strain is found to be 0.2%. In both panels, the grey window shows the range of average load values τ_0 wherein creep is linear.

Aging and rejuvenation in C–S–H under stress perturbations. We now assess the influence of the amplitude of the stress perturbations used herein to accelerate the dynamics of C–S–H under creep. Figure 5a shows the creep modulus value *C* (computed under a constant shear stress of 100 MPa, i.e., in the linear regime) as a function of the amplitude of the stress perturbation $\Delta\tau$. We observe that, for low values of $\Delta\tau$, the obtained creep modulus remains largely constant. This indicates that, in this regime, the creep modulus value yielded by our methodology is not affected by the specific choice of $\Delta\tau$—which is an important observation that confirms the reliability of our approach.

However, we observe that *C* suddenly increases when $\Delta\tau$ becomes larger than a threshold value (found to be around 45 MPa herein). This indicates that the accelerated creep of the system is only achieved over a certain range of stress perturbation magnitude (i.e., less than 45 MPa). In contrast, larger values of stress perturbation amplitude do not result in any significant creep deformation, which manifests itself by an increase in *C*—i.e., an increase in the apparent resistance to creep under fixed external load.

This observation can be understood as a balance between stress-induced overaging and rejuvenation. Indeed, as mentioned above, it has been observed that the application of a small stress tends to make a system overage (i.e., accelerate the spontaneous aging of an out-of-equilibrium system) by deforming the energy landscape and suppressing some preexisting energy barriers [40,46]. In turn, the application of a large stress can induce some rejuvenation by significantly moving the system away from its initial position in the energy landscape [8,40,46]. To demonstrate the effect, we compute the potential energy U of a monodisperse C–S–H system having experienced upon creep a constant shear strain deformation (γ = 0.2%). Figure 5b shows the evolution of U as a function of the stress perturbation amplitude $\Delta\tau$ used to stimulate creep. We observe that, for small values of $\Delta\tau$ (i.e. less than 45 MPa), the energy of the system remains fairly independent of $\Delta\tau$. In contrast, for larger values of $\Delta\tau$, we observe a significant increase in U. This confirms that large values of stress perturbations amplitude results in a rejuvenation of the system, that is, a destabilization toward higher energy states. This *a posteriori* confirms that the energy state of the system experiencing creep is not affected by the choice of $\Delta\tau$ as long as no rejuvenation is induced.

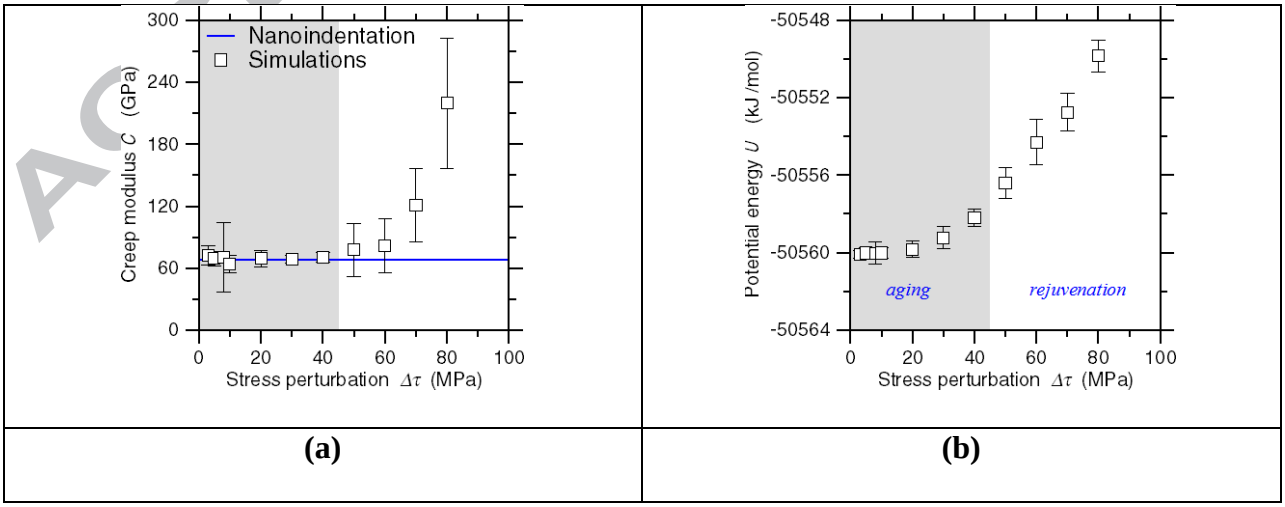

(a) **(b)**

Fig. 5: (a) Computed creep modulus *C* (see Eq. 3) in monodisperse colloidal C–S–H gels under varying stress perturbation amplitudes $\Delta\tau$ (for τ_0 = 100 MPa). The results are compared with experimental nanoindentation data (blue line) [11,42]. (b) Computed molar potential energy of monodisperse colloidal C–S–H gels at fixed shear strain deformation (γ = 0.2%) under select stress perturbation amplitudes $\Delta\tau$ (for τ_0 = 100 MPa). In both panels, the grey window shows the range of $\Delta\tau$ values wherein *C* is constant.

Experimental validation of our accelerated simulation technique. Having established the range of $\Delta\tau$ values for which our methodology yield an accelerated creep dynamics without inducing any rejuvenation, we are now in position to compare our computed results with those obtained experimentally. Note that such a direct comparison may be challenging due to the fact that the state of stress experienced in experiments (e.g., nanoindentation) can significantly differ from that imposed herein. Nevertheless, the fact that (i) the value of the creep modulus and (ii) the nature of the mapping between number of stress cycles and corresponding creep time both do not depend on the applied load (see Sec. 3.2) makes it possible to meaningfully compare computed and experimental data.

Based on these observations, we now assess the effect of the packing density of C–S–H on its creep modulus and compare the outcome to nanoindentation data [11,42]. The nanoindentation experiments—whose outcomes are used herein to validate our simulations—were conducted on cementitious binders formed upon the hydration of ordinary portland cement [11]. The creep modulus was determined by applying a constant load and measuring the time-dependent displacement of the indenter. A clustering algorithm was used to isolate the properties of C–S–H from those of the other phases [11]. Figure 6a shows the shear strain exhibited by C–

S–H configurations for select packing density values. Overall, we observe the conclusions previously established in the case of monodisperse C–S–H are retained for polydisperse systems, namely, (i) creep exhibits a logarithmic dependence on time, (ii) creep is load-linear as long as the applied stress remains smaller than the yield stress of the system, and (iii) the value of the computed creep modulus is independent of the amplitude of the stress perturbations as long as no rejuvenation is induced. This allows us to compute the evolution of the creep modulus as a function of packing density following Eq. 3. As shown in Fig. 6b, we observe that the creep modulus increases with increasing values of C–S–H packing density. Importantly, we obtain an excellent agreement between simulation and nanoindentation data [11,42], which strongly supports the ability of our model and accelerated simulation method to offer a realistic description of the creep of C–S–H.

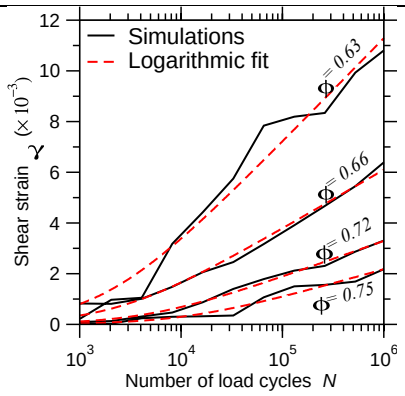

(a)

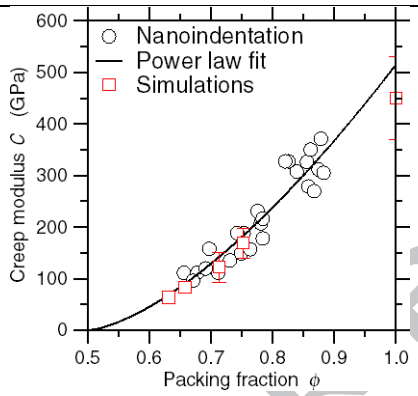

(b)

Fig. 6: (a) Computed shear strain in polydisperse colloidal C–S–H gels with respect to the number of stress perturbation cycles and for select packing densities ϕ (with τ_0 = 100 MPa and $\Delta\tau$ = 30 MPa). The dashed lines are some logarithmic fits (see Eq. 3). (b) Computed creep modulus C (see Eq. 3) of C–S–H as a function of the packing fraction. The results are compared with experimental nanoindentation data [11] and data from a previous atomistic simulation of creep in bulk C–S–H at ϕ = 1, that is, with no porosity [6]. The solid line is a power-law fit (see Eq. 4).

Discussion

The good agreement between the creep modulus data presented in Fig. 6b with nanoindentation suggests that the mesoscale model of C–S–H is able to properly capture the mechanism of creep in C–S–H and, in turn, that other features that are not considered by the present model do not necessarily need to be accounted for to model C–S–H creep (see below). This shows that, under load, the creep of C–S–H occurs via some structural reorganization within the mesoscale structure of C–S–H. Specifically, the fact that our mesoscale model of C–S–H is based on grains of constant geometry suggests that creep does not arise from time-dependent

variations in the volume or shape of the C–S–H grains, but rather arise from some reorganization in the mesoscale structure of the grains. Nevertheless, such mesoscale rearrangements necessarily occur through some atomic-scale deformations at the interface between C–S–H grains. Then, the fact that the present mesoscale model yields some creep modulus values that are in good agreement with experiments although it only considers spherical grains suggests the shape of the grains may not have a first-order effect on the height of the energy barriers that need to be overcome upon creep. In addition, since the present mesoscale model relies on a spherical, isotropic description of the C–S–H grains, our results suggest that the relative orientation of the C–S–H grains with respect to each other may not affect creep to the first order—which may arise from the fact that the local packing density has a first order effect in controlling the magnitude of the energy barriers in such dense systems. Finally, the fact that our model does not incorporate any transversal force opposing the sliding among particles suggests that frictional and shearing effects acting the level of the interlayer space in the C–S–H grains are not necessarily the sole or main factor responsible for creep of C–S–H, which in agreement with previous studies [47,48].

Overall, our results suggest that the nature of C–S–H creep is primarily nanogranular. This is also supported by the logarithmic time-evolution of creep (see Sec. 3.1), which can elegantly be explained by the free-volume theory (FVT) in granular physics. In details, FVT assumes that the creep/aging of the system occurs via some structural reorganization of the grains that jump into some local free space—so that the changing rate of the packing density $\dot{\phi}$ (and, hence, the creep deformation rate $\dot{\gamma}$) is expected to be proportional to the amount of holes that are larger than the grain size. It is then assumed that that size of the holes (i.e., local free volume Ω) exhibits a Poisson's distribution $p(\Omega) = \frac{1}{\theta}\exp(-\Omega/\theta)$, wherein θ the average free volume per grain. The normalized amount of accessible holes per jumping grain can be expressed as the

probability of holes that are larger than the grain size (ρ), that is, $\int_{\rho}^{\infty} p(\Omega)\, d\Omega = \exp(-\rho/\theta)$. As such, FVT predicts that the deformation rate $\dot{\phi}$ decreases exponentially as a function of the excluded volume θ, i.e., $\dot{\phi} \propto \exp(-\rho/\theta)$. Further, one gets $\theta = \rho(1/\phi - 1/\phi_\infty) \approx \rho{\phi_\infty}^{-2}(\phi_\infty - \phi)$, wherein ϕ represents the packing density of current aging system and ϕ_∞ is the ultimately limit packing density (note that, at the vicinity of the jamming threshold, $|\phi_\infty - \phi| \ll 1$). Finally, the time integration of $\dot{\phi} \propto \exp(-\rho/\theta)$ yields $t \propto \exp(\rho/\theta)$, so that $\dot{\phi} \propto t^{-1}$ [11,27].

The nanogranular nature of C–S–H's creep is also supported by the dependence of the creep modulus on the packing density (see Fig. 6b). In details, we find that the evolution of the creep modulus can be well described by a power law: [11,42]

$$C = C_0 \times (2\phi - 1)^{\alpha} \qquad \textbf{(Eq. 4)}$$

where α is the power law exponent and C_0 the value of the creep modulus at zero porosity (i.e., $\phi = 1$). This trend can be understood from the fact that C–S–H must exhibit a minimum packing fraction that is larger than 0.5 to present a percolated structure featuring a non-zero stiffness, hardness, and resistance to creep [9,29]. Starting from this threshold, the increase in *C* (i.e., increase in C–S–H's resistance to creep) with increasing packing density is consistent with the free-volume theory framework [27]—since the level of free space (θ) accessible to the C–S–H grains decreases upon increasing packing density ϕ. In details, the relationship:

$$\dot{\phi} \propto \exp(-\rho/\theta) = \exp\left[-(1/\phi - 1/\phi_\infty)^{-1}\right] \qquad \textbf{(Eq. 5)}$$

established above based on the FVT framework suggests that the deformation rate $\dot{\phi}$ decreases (and, therefore, that the resistance to creep *C* increases) with increasing packing density. From a

mechanism viewpoint, this trend suggests that, by filling the existing free space left in the mesostructure, the presence of small C–S–H grains in between the larger C–S–H grains effectively reduces the number of possible structural reorganizations and, thereby, reduces the propensity for creep. Finally, it should be pointed out that, although our results are consistent with free-volume theory, our simulations do not exclude other possible physical origins. Clearly, more work is needed to further investigate the nature of the structural reorganization occurring during creep.

Note that the present results do not involve that the atomic structure and composition of the C–S–H grains is irrelevant. Actually, these atomic details are already embedded in the effective potential energy governing the mutual interactions between each pair of C–S–H grains (following Eq. 1). Namely, a variation in the atomic composition and structure of the C–S–H grains would affect the values of the parameters used in Eq. 1, which, in turn, would change the dynamics of creep. In fact, the role of the atomic scale is captured in the C_0 term in Eq. 4, that is, the creep modulus at zero porosity (i.e., in the absence of any free volume). Notably, the creep modulus at zero porosity that can here be obtained by extrapolating our computed results toward $\phi = 1$ is in very good agreement with the data predicted by atomic-scale molecular dynamics simulations (see Fig. 6b) [6,15]. This highlights the importance of both the atomic and mesoscale structure in controlling the creep of cementitious binders.

Conclusions

To summarize, by accelerating the aging of the C–S–H mesostructure when subjected to a sustained load, our accelerated simulation method can properly describe the long-term creep of C–S–H and yield a quantitative agreement with experimental nanoindentation data. We observe

that the creep of C–S–H exhibit a logarithmic dependence on time and a linear dependence on the applied load—which supports the nanogranular nature of C–S–H creep. Importantly, this work offers the first consistent description of the effect of packing on the propensity for creep of C–S–H. Our modeling framework now makes it possible to further investigate the structural mechanism of creep in C–S–H gels, explore the potential for the discovery of creep-resistant structures, and investigate the effect of each of the hypothesis/parameters of our model. From a practical viewpoint, our methodology can be used to predict the long-term creep deformation of C–S–H gels, which is challenging to access experimentally due to associated time and length scales [11,42]. More generally, our accelerated aging methodology is generic and can be applied to investigate the mechanism(s) governing the relaxation of out-of-equilibrium phases, e.g., glassy, colloidal, or granular materials.

Acknowledgements

This work was supported by the National Science Foundation under Grant No. 1562066.

References

[1] V. Trappe, V. Prasad, L. Cipelletti, P.N. Segre, D.A. Weitz, Jamming phase diagram for attractive particles, Nature. 411 (2001) 772–775. doi:10.1038/35081021.

[2] M.Y. Lin, H.M. Lindsay, D.A. Weitz, R.C. Ball, R. Klein, P. Meakin, Universality in colloid aggregation, Nature. 339 (1989) 360–362. doi:10.1038/339360a0.

[3] Y.M. Joshi, Dynamics of Colloidal Glasses and Gels, Annual Review of Chemical and Biomolecular Engineering. 5 (2014) 181–202. doi:10.1146/annurev-chembioeng-060713-040230.

[4] Wang Q., Wang L., Detamore M. S., Berkland C., Biodegradable Colloidal Gels as Moldable Tissue Engineering Scaffolds, Advanced Materials. 20 (2007) 236–239. doi:10.1002/adma.200702099.

[5] E. Masoero, E. Del Gado, R.J.-M. Pellenq, F.-J. Ulm, S. Yip, Nanostructure and Nanomechanics of Cement: Polydisperse Colloidal Packing, Phys. Rev. Lett. 109 (2012) 155503. doi:10.1103/PhysRevLett.109.155503.

[6] M. Bauchy, M. Wang, Y. Yu, B. Wang, N.M.A. Krishnan, E. Masoero, F.-J. Ulm, R. Pellenq, Topological Control on the Structural Relaxation of Atomic Networks under Stress, Physical Review Letters. 119 (2017). doi:10.1103/PhysRevLett.119.035502.

[7] D.J. Lacks, Energy Landscapes and the Non-Newtonian Viscosity of Liquids and Glasses, Physical Review Letters. 87 (2001). doi:10.1103/PhysRevLett.87.225502.

[8] D.J. Lacks, M.J. Osborne, Energy Landscape Picture of Overaging and Rejuvenation in a Sheared Glass, Physical Review Letters. 93 (2004). doi:10.1103/PhysRevLett.93.255501.

[9] K. Ioannidou, K.J. Krakowiak, M. Bauchy, C.G. Hoover, E. Masoero, S. Yip, F.-J. Ulm, P. Levitz, R.J.-M. Pellenq, E.D. Gado, Mesoscale texture of cement hydrates, PNAS. 113 (2016) 2029–2034. doi:10.1073/pnas.1520487113.

[10] H.M. Jennings, Refinements to colloid model of C-S-H in cement: CM-II, Cement and Concrete Research. 38 (2008) 275–289. doi:10.1016/j.cemconres.2007.10.006.

[11] M. Vandamme, F.-J. Ulm, Nanogranular origin of concrete creep, PNAS. 106 (2009) 10552–10557. doi:10.1073/pnas.0901033106.

[12] Z. Bažant, M. Hubler, R. Wendner, Q. Yu, Progress in Creep and Shrinkage Prediction Engendered by Alarming Bridge Observations and Expansion of Laboratory Database, in: Mechanics and Physics of Creep, Shrinkage, and Durability of Concrete, American Society

of Civil Engineers, 2013: pp. 1–17. http://ascelibrary.org/doi/abs/10.1061/9780784413111.001 (accessed December 18, 2014).

[13] Z.P. Bažant, M.H. Hubler, Q. Yu, Excessive creep deflections: An awakening, Concrete International. 33 (2011) 44–46.

[14] H.M. Jennings, Colloid model of C−S−H and implications to the problem of creep and shrinkage, Mat. Struct. 37 (2004) 59–70. doi:10.1007/BF02481627.

[15] I. Pignatelli, A. Kumar, R. Alizadeh, Y.L. Pape, M. Bauchy, G. Sant, A dissolution-precipitation mechanism is at the origin of concrete creep in moist environments, The Journal of Chemical Physics. 145 (2016) 054701. doi:10.1063/1.4955429.

[16] H. Liu, T. Du, N.M.A. Krishnan, H. Li, M. Bauchy, Topological optimization of cementitious binders: Advances and challenges, Cement and Concrete Composites. (2018). doi:10.1016/j.cemconcomp.2018.08.002.

[17] C. Le Quéré, R.J. Andres, T. Boden, T. Conway, R.A. Houghton, J.I. House, G. Marland, G.P. Peters, G. van der Werf, A. Ahlström, R.M. Andrew, L. Bopp, J.G. Canadell, P. Ciais, S.C. Doney, C. Enright, P. Friedlingstein, C. Huntingford, A.K. Jain, C. Jourdain, E. Kato, R.F. Keeling, K. Klein Goldewijk, S. Levis, P. Levy, M. Lomas, B. Poulter, M.R. Raupach, J. Schwinger, S. Sitch, B.D. Stocker, N. Viovy, S. Zaehle, N. Zeng, The global carbon budget 1959–2011, Earth System Science Data Discussions. 5 (2012) 1107–1157. doi:info:doi:10.5194/essdd-5-1107-2012.

[18] M. Bauchy, Nanoengineering of concrete via topological constraint theory, MRS Bulletin. 42 (2017) 50–54. doi:10.1557/mrs.2016.295.

[19] Z. Bažant, S. Prasannan, Solidification Theory for Concrete Creep. I: Formulation, Journal of Engineering Mechanics. 115 (1989) 1691–1703. doi:10.1061/(ASCE)0733-9399(1989)115:8(1691).

[20] Z. Bažant, A. Hauggaard, S. Baweja, F. Ulm, Microprestress-Solidification Theory for Concrete Creep. I: Aging and Drying Effects, Journal of Engineering Mechanics. 123 (1997) 1188–1194. doi:10.1061/(ASCE)0733-9399(1997)123:11(1188).

[21] R. Sinko, M. Vandamme, Z.P. Bažant, S. Keten, Transient effects of drying creep in nanoporous solids: understanding the effects of nanoscale energy barriers, Proc. R. Soc. A. 472 (2016) 20160490. doi:10.1098/rspa.2016.0490.

[22] A. Morshedifard, S. Masoumi, M.J.A. Qomi, Nanoscale origins of creep in calcium silicate hydrates, Nature Communications. 9 (2018) 1785. doi:10.1038/s41467-018-04174-z.

[23] M.J.A. Qomi, E. Masoero, M. Bauchy, F.-J. Ulm, E.D. Gado, R.J.-M. Pellenq, C-S-H across Length Scales: From Nano to Micron, in: CONCREEP 10, American Society of Civil Engineers, n.d.: pp. 39–48. http://ascelibrary.org/doi/abs/10.1061/9780784479346.006 (accessed July 3, 2016).

[24] Y. Yu, M. Wang, D. Zhang, B. Wang, G. Sant, M. Bauchy, Stretched Exponential Relaxation of Glasses at Low Temperature, Physical Review Letters. 115 (2015). doi:10.1103/PhysRevLett.115.165901.

[25] G.T. Barkema, N. Mousseau, Event-Based Relaxation of Continuous Disordered Systems, Physical Review Letters. 77 (1996) 4358–4361. doi:10.1103/PhysRevLett.77.4358.

[26] Y. Yu, M. Wang, M.M. Smedskjaer, J.C. Mauro, G. Sant, M. Bauchy, Thermometer Effect: Origin of the Mixed Alkali Effect in Glass Relaxation, Phys. Rev. Lett. 119 (2017) 095501. doi:10.1103/PhysRevLett.119.095501.

[27] T. Boutreux, P.G. de Geennes, Compaction of granular mixtures: a free volume model, Physica A: Statistical Mechanics and Its Applications. 244 (1997) 59–67. doi:10.1016/S0378-4371(97)00236-7.

[28] E. Masoero, E.D. Gado, R. J.-M. Pellenq, S. Yip, F.-J. Ulm, Nano-scale mechanics of colloidal C–S–H gels, Soft Matter. 10 (2014) 491–499. doi:10.1039/C3SM51815A.

[29] H. Liu, S. Dong, L. Tang, N.M.A. Krishnan, G. Sant, M. Bauchy, Effects of Polydispersity and Disorder on the Mechanical Properties of Hydrated Silicate Gels. Journal of the Mechanics and Physics of Solids. 122 (2019) 555–565. doi: 10.1016/j.jmps.2018.10.003.

[30] H. Manzano, E. Masoero, I. Lopez-Arbeloa, H. M. Jennings, Shear deformations in calcium silicate hydrates, Soft Matter. 9 (2013) 7333–7341. doi:10.1039/C3SM50442E.

[31] H. Manzano, S. Moeini, F. Marinelli, A.C.T. van Duin, F.-J. Ulm, R.J.-M. Pellenq, Confined Water Dissociation in Microporous Defective Silicates: Mechanism, Dipole Distribution, and Impact on Substrate Properties, J. Am. Chem. Soc. 134 (2012) 2208–2215. doi:10.1021/ja209152n.

[32] H. Liu, L. Tang, N.M.A. Krishnan, G. Sant, B. Mathieu, Structural Percolation Controls the Precipitation Kinetics of Colloidal Calcium–Silicate–Hydrate Gels. (n.d.).

[33] K. Ioannidou, M. Kanduč, L. Li, D. Frenkel, J. Dobnikar, E. Del Gado, The crucial effect of early-stage gelation on the mechanical properties of cement hydrates, Nature Communications. 7 (2016) 12106. doi:10.1038/ncomms12106.

[34] K. Ioannidou, R. J.-M. Pellenq, E.D. Gado, Controlling local packing and growth in calcium–silicate–hydrate gels, Soft Matter. 10 (2014) 1121–1133. doi:10.1039/C3SM52232F.

[35] D. Frenkel, B. Smit, Understanding Molecular Simulation: From Algorithms to Applications, Elsevier, 2001.

[36] M. Hermes, M. Dijkstra, Jamming of polydisperse hard spheres: The effect of kinetic arrest, EPL. 89 (2010) 38005. doi:10.1209/0295-5075/89/38005.

[37] A. Donev, I. Cisse, D. Sachs, E.A. Variano, F.H. Stillinger, R. Connelly, S. Torquato, P.M. Chaikin, Improving the Density of Jammed Disordered Packings Using Ellipsoids, Science. 303 (2004) 990–993. doi:10.1126/science.1093010.

[38] G.D. Scott, D.M. Kilgour, The density of random close packing of spheres, J. Phys. D: Appl. Phys. 2 (1969) 863. doi:10.1088/0022-3727/2/6/311.

[39] P. Richard, M. Nicodemi, R. Delannay, P. Ribière, D. Bideau, Slow relaxation and compaction of granular systems, Nature Materials. 4 (2005) 121–128. doi:10.1038/nmat1300.

[40] M. Utz, P.G. Debenedetti, F.H. Stillinger, Atomistic Simulation of Aging and Rejuvenation in Glasses, Physical Review Letters. 84 (2000) 1471–1474. doi:10.1103/PhysRevLett.84.1471.

[41] G.G. Naumis, Energy landscape and rigidity, Phys. Rev. E. 71 (2005) 026114. doi:10.1103/PhysRevE.71.026114.

[42] M. Vandamme, F.-J. Ulm, Nanoindentation investigation of creep properties of calcium silicate hydrates, Cement and Concrete Research. 52 (2013) 38–52. doi:10.1016/j.cemconres.2013.05.006.

[43] M. Davis, N. Thompson, Creep in a Precipitation-Hardened Alloy, Proc. Phys. Soc. B. 63 (1950) 847. doi:10.1088/0370-1301/63/11/303.

[44] T.W. Lambe, R.V. Whitman, Soil mechanics. Massachusetts institute of technology, John Wiley and Sons, New York, 1969.

[45] E. Masoero, M. Bauchy, E. Del Gado, H. Manzano, R.M. Pellenq, F.-J. Ulm, S. Yip, Kinetic Simulations of Cement Creep: Mechanisms from Shear Deformations of Glasses, in: CONCREEP 10, American Society of Civil Engineers, Vienna, Austria, 2015: pp. 555–564. doi:10.1061/9780784479346.068.

[46] V. Viasnoff, F. Lequeux, Rejuvenation and Overaging in a Colloidal Glass under Shear, Phys. Rev. Lett. 89 (2002) 065701. doi:10.1103/PhysRevLett.89.065701.

[47] P. Klug, F. Wittmann, Activation energy of creep of hardened cement paste, Matériaux et Constructions. 2 (1969) 11–16. doi:10.1007/BF02473650.

[48] P Klug and F Wittmann. Activation energy and activation volume of creep of hardened cement paste. Materials science and Engineering. 15 (1974) 63–66. doi: 10.1016/0025-5416(74)90030-5.